

Direct Production of Light Scalar in the Type-I Two-Higgs-Doublet Model at the Lifetime Frontier of LHC

Wei Liu,^a Lei Wang,^b and Yu Zhang^c

^a*Department of Applied Physics and MIIT Key Laboratory of Semiconductor Microstructure and Quantum Sensing, Nanjing University of Science and Technology, Nanjing 210094, China*

^b*Department of Physics, Yantai University, Yantai 264005, P. R. China*

^c*School of Physics, Hefei University of Technology, Hefei 230601, China*

E-mail: wei.liu@njust.edu.cn, leiwang@ytu.edu.cn, dayu@hfut.edu.cn

ABSTRACT: A light pseudoscalar A in the sufficient large $\tan\beta$ region of type-I two-Higgs-doublet model (2HDM) can be naturally a long-lived particle (LLP). We focus on the $H^\pm A$, HA and AA pair productions via the electroweak processes mediated by the bosons at the LHC, including $pp \rightarrow W^\pm/Z \rightarrow H^\pm/HA$ and $pp \rightarrow h \rightarrow AA$ at the 14 TeV LHC. The possibility of probing A as a LLP at the FASER-2, FACET, MoEDAL-MAPP-2, MATHUSLA is discussed. We find that FASER-2 fails to probe any parameter space within $0.2 \text{ GeV} < m_A < 10 \text{ GeV}$ for both processes. For $130 < m_{H^\pm} = m_H < 400 \text{ GeV}$, FACET, MoEDAL-MAPP-2 and MATHUSLA can probes $\tan\beta \lesssim 10^{4-6}$ for $m_A \lesssim 3 \text{ GeV}$, and $\tan\beta \lesssim 10^{6-8}$ for $3 \text{ GeV} \lesssim m_A < 10 \text{ GeV}$ from $pp \rightarrow W^\pm/Z \rightarrow H^\pm/ZA$ processes. And $pp \rightarrow h \rightarrow AA$ covers similar parameter space. All processes can surpass the current limits.

Contents

1	Introduction	1
2	Type-I of two-Higgs-doublet model	2
3	Relevant theoretical and experimental constraints	4
4	The detection of A as a long-lived particle	6
5	Conclusion	13

1 Introduction

After the discovery of the Higgs boson at the LHC [1, 2], searching for extra Higgs becomes an important task. In contrast to the main detectors at the the Large Hadron Collider (LHC), such as ATLAS and CMS, which often focus on searching for heavy resonance states with the mass larger than several hundreds GeV or even few TeV, there has been a growing interest in lighter feebly interacting particles with the mass of $\mathcal{O}(\text{GeV})$. These particles typically possess longer lifetimes, enabling them to escape the main detector.

Aiming for detecting long-lived particles (LLPs), a series proposal of dedicated detectors based on the LHC have been put forward, including FASER [3, 4], FACET [5], MoEDAL-MAPP (MAPP) [6, 7], MATHUSLA [8], ANUBIS [9], Codex-b [10], AL3X [11], etc. Among them, FASER and MAPP have already been installed and performing searches starting at the Run 3 of the LHC. These detectors have shown ample potential to probe LLPs including dark matter [12–16], hidden valley [17, 18], dark photon [19–22], axion-like particles [23–26], heavy neutrinos [27–43], and vector-like lepton [44, 45]. Light scalars can also be potentially discovered at these detectors [46–48].

From the theory side, many models include extended scalar sector, like the popular two-Higgs-doublet model (2HDM). The 2HDM model [49] is a simple extension of SM by adding a second $SU(2)_L$ Higgs doublet, which has very rich Higgs phenomenology, including two neutral CP-even Higgs bosons h and H , one neutral pseudoscalar A , and a pair of charged Higgs H^\pm . According to the different Yukawa couplings, there are four types for 2HDMs which prevent the tree-level flavor changing neutral currents, the type-I [50, 51], type-II [50, 52], lepton-specific, and flipped models [53–56].

In this paper, we will focus on the type-I 2HDM, in which the long-lived scalar A can be searched at FASER, FACET, MAPP and MATHUSLA. Its couplings with the fermion pairs are proportional to the ratio of the two vacuum expectation value, $1/\tan\beta$ which can be tiny. Given it is light, it can be long-lived. Therefore, it becomes an ideal candidates of LLP, which has been widely searched at the LHC in recent years [57].

In Ref. [46] the authors studied FASER and FASER 2 reaches of A as a LLP which is produced from meson decays. The final states are flying in a very forward direction, where FASER is located, hence have shown complimentary sensitivity to A . In this paper, we change the strategy, by searching for the A via mediated bosons, such as $pp \rightarrow W^\pm/Z \rightarrow H^\pm/HA$ and $pp \rightarrow h \rightarrow AA$. The decay products are expected to distributed in a more transverse direction, hence not only the forward detectors including FASER-2 and FACET, but also MAPP-2, MATHUSLA can potentially probe A .

This paper is organised as follows, in section 2, we briefly introduce the type-I of 2HDM model. The relevant theoretical and experimental constraints on the mass of the A , m_A and $\tan\beta$, is summarised in section 3. In section 4, we show the sensitivity of the same parameter space by searching for A at LLP detectors. Finally, the conclusion is drawn in section 5.

2 Type-I of two-Higgs-doublet model

In the type-I 2HDM, the Higgs potential with a soft Z_2 symmetry breaking can be written as

$$\begin{aligned} \mathcal{V}_{tree} = & m_{11}^2(\Phi_1^\dagger\Phi_1) + m_{22}^2(\Phi_2^\dagger\Phi_2) - \left[m_{12}^2(\Phi_1^\dagger\Phi_2 + \text{h.c.}) \right] \\ & + \frac{\lambda_1}{2}(\Phi_1^\dagger\Phi_1)^2 + \frac{\lambda_2}{2}(\Phi_2^\dagger\Phi_2)^2 + \lambda_3(\Phi_1^\dagger\Phi_1)(\Phi_2^\dagger\Phi_2) + \lambda_4(\Phi_1^\dagger\Phi_2)(\Phi_2^\dagger\Phi_1) \\ & + \left[\frac{\lambda_5}{2}(\Phi_1^\dagger\Phi_2)^2 + \text{h.c.} \right]. \end{aligned} \quad (2.1)$$

We consider a CP-conserving case in which all λ_i and m_{12}^2 are real. The two complex Higgs doublet fields Φ_1 and Φ_2 have hypercharge $Y = 1$ and are expanded as

$$\Phi_1 = \begin{pmatrix} \phi_1^+ \\ \frac{1}{\sqrt{2}}(v_1 + \phi_1 + ia_1) \end{pmatrix}, \quad \Phi_2 = \begin{pmatrix} \phi_2^+ \\ \frac{1}{\sqrt{2}}(v_2 + \phi_2 + ia_2) \end{pmatrix}, \quad (2.2)$$

with v_1 and v_2 being the electroweak vacuum expectation values (VEVs) and $v^2 = v_1^2 + v_2^2 = (246 \text{ GeV})^2$. We define the ratio of the two VEVs as $\tan\beta = v_2/v_1$. After spontaneous electroweak symmetry breaking, the mass eigenstates are obtained from the original fields by the rotation matrices,

$$\begin{pmatrix} H \\ h \end{pmatrix} = \begin{pmatrix} \cos\alpha & \sin\alpha \\ -\sin\alpha & \cos\alpha \end{pmatrix} \begin{pmatrix} \phi_1 \\ \phi_2 \end{pmatrix}, \quad (2.3)$$

$$\begin{pmatrix} G^0 \\ A \end{pmatrix} = \begin{pmatrix} \cos\beta & \sin\beta \\ -\sin\beta & \cos\beta \end{pmatrix} \begin{pmatrix} a_1 \\ a_2 \end{pmatrix}, \quad (2.4)$$

$$\begin{pmatrix} G^\pm \\ H^\pm \end{pmatrix} = \begin{pmatrix} \cos\beta & \sin\beta \\ -\sin\beta & \cos\beta \end{pmatrix} \begin{pmatrix} \phi_1^\pm \\ \phi_2^\pm \end{pmatrix}. \quad (2.5)$$

The G^0 and G^\pm are Goldstones which are eaten by gauge bosons Z and W^\pm . The remaining physical states are two neutral CP-even states h, H , one neutral pseudoscalar A , and a pair

of charged scalars H^\pm . Taking the Higgs masses as the input parameters, the coupling constants in the Higgs potential are expressed by

$$\begin{aligned} v^2 \lambda_1 &= \frac{m_H^2 c_\alpha^2 + m_h^2 s_\alpha^2 - m_{12}^2 t_\beta}{c_\beta^2}, & v^2 \lambda_2 &= \frac{m_H^2 s_\alpha^2 + m_h^2 c_\alpha^2 - m_{12}^2 t_\beta^{-1}}{s_\beta^2}, \\ v^2 \lambda_3 &= \frac{(m_H^2 - m_h^2) s_\alpha c_\alpha + 2m_{H^\pm}^2 s_\beta c_\beta - m_{12}^2}{s_\beta c_\beta}, & v^2 \lambda_4 &= \frac{(m_A^2 - 2m_{H^\pm}^2) s_\beta c_\beta + m_{12}^2}{s_\beta c_\beta}, \\ v^2 \lambda_5 &= \frac{-m_A^2 s_\beta c_\beta + m_{12}^2}{s_\beta c_\beta}, \end{aligned} \quad (2.6)$$

where the shorthand notations $s_\beta \equiv \sin \beta$ and $c_\beta \equiv \cos \beta$. When $\sin(\beta - \alpha)$ is very closed to 1.0, we can approximately obtain the following relations,

$$\begin{aligned} v^2 \lambda_1 &= m_h^2 - \frac{t_\beta^3 (m_{12}^2 - m_H^2 s_\beta c_\beta)}{s_\beta^2}, \\ v^2 \lambda_2 &= m_h^2 - \frac{(m_{12}^2 - m_H^2 s_\beta c_\beta)}{t_\beta s_\beta^2}, \\ v^2 \lambda_3 &= m_h^2 + 2m_{H^\pm}^2 - 2m_H^2 - \frac{t_\beta (m_{12}^2 - m_H^2 s_\beta c_\beta)}{s_\beta^2}, \\ v^2 \lambda_4 &= m_A^2 - 2m_{H^\pm}^2 + m_H^2 + \frac{t_\beta (m_{12}^2 - m_H^2 s_\beta c_\beta)}{s_\beta^2}, \\ v^2 \lambda_5 &= m_H^2 - m_A^2 + \frac{t_\beta (m_{12}^2 - m_H^2 s_\beta c_\beta)}{s_\beta^2}. \end{aligned} \quad (2.7)$$

The Yukawa interactions of type-I model are

$$-\mathcal{L} = Y_{u2} \bar{Q}_L \tilde{\Phi}_2 u_R + Y_{d2} \bar{Q}_L \Phi_2 d_R + Y_{\ell 2} \bar{L}_L \Phi_2 e_R + \text{h.c.} \quad (2.8)$$

where $Q_L^T = (u_L, d_L)$, $L_L^T = (\nu_L, l_L)$, $\tilde{\Phi}_{1,2} = i\tau_2 \Phi_{1,2}^*$, and Y_{u2} , $Y_{d1,d2}$ and $Y_{\ell 1,\ell 2}$ are 3×3 matrices in family space.

The Yukawa couplings of the neutral Higgs bosons with respect to the SM are

$$\begin{aligned} y_h^{f_i} &= [\sin(\beta - \alpha) + \cos(\beta - \alpha) \kappa_f], \\ y_H^{f_i} &= [\cos(\beta - \alpha) - \sin(\beta - \alpha) \kappa_f], \\ y_A^{f_i} &= -i\kappa_f \text{ (for } u), \quad y_A^{f_i} = i\kappa_f \text{ (for } d, \ell), \\ &\text{with } \kappa_d = \kappa_\ell = \kappa_u \equiv 1/\tan \beta \text{ for type-I.} \end{aligned} \quad (2.9)$$

The Yukawa interactions of the charged Higgs are

$$\mathcal{L}_Y = -\frac{\sqrt{2}}{v} H^+ \left\{ \bar{u}_i [\kappa_d (V_{CKM})_{ij} m_{dj} P_R - \kappa_u m_{ui} (V_{CKM})_{ij} P_L] d_j + \kappa_\ell \bar{\nu} m_\ell P_R \ell \right\} + \text{h.c.}, \quad (2.10)$$

where $i, j = 1, 2, 3$. The neutral Higgs boson couplings with the gauge bosons normalized to the SM are

$$y_h^V = \sin(\beta - \alpha), \quad y_H^V = \cos(\beta - \alpha), \quad (2.11)$$

where $V = Z, W$. The pseudoscalar A has no couplings to V because of the CP-conserving.

3 Relevant theoretical and experimental constraints

We take the light CP-even Higgs boson h as the observed 125 GeV Higgs, and assume the approximate alignment limit, namely $|\sin(\beta - \alpha)| \rightarrow 1$, which can ensure that the tree-level coupling of h to the SM particles are very closed to the SM. As a light LLP, the $h \rightarrow AA$ is restricted by the invisible Higgs decay of $Br(h \rightarrow \text{invisible}) < 0.24$ [58–60]. In addition, the diphoton channel provides the most precise measurement on the property of the 125 GeV Higgs, and the signal strength imposes a stringent bound [61]

$$\mu_{\gamma\gamma} = 1.11^{+0.10}_{-0.09}. \quad (3.1)$$

In the model, the one-loop diagrams of the charged Higgs can give additional contributions to the $h \rightarrow \gamma\gamma$ decay [62], and the $h \rightarrow AA$ enhances the total width of h . Therefore, the diphoton signal strength can constrain the parameter space of the model strongly.

We consider theoretical constraints of vacuum stability, perturbativity and unitarity. To maintain the perturbativity of theory, we demand the quartic Higgs couplings to be smaller than 4π . The conditions of vacuum stability are [63]

$$\lambda_1 > 0, \quad \lambda_2 > 0, \quad \lambda_3 + \sqrt{\lambda_1 \lambda_2} > 0, \quad \lambda_3 + \lambda_4 - |\lambda_5| + \sqrt{\lambda_1 \lambda_2} > 0. \quad (3.2)$$

Tree-Level perturbative unitarity conditions ensures perturbativity of the model up to very high scales, which demands that the amplitudes of the scalar quartic interactions leading to $2 \rightarrow 2$ scattering processes remain below the value of 8π at tree-level. The requirement leads to the constraints [64, 65],

$$|a_{\pm}|, |b_{\pm}|, |c_{\pm}|, |e_{\pm}|, |f_{\pm}|, |g_{\pm}| \leq 8\pi \quad (3.3)$$

with

$$\begin{aligned} a_{\pm} &= \frac{3}{2}(\lambda_1 + \lambda_2) \pm \sqrt{\frac{9}{4}(\lambda_1 - \lambda_2)^2 + (2\lambda_3 + \lambda_4)^2}, \\ b_{\pm} &= \frac{1}{2}(\lambda_1 + \lambda_2) \pm \sqrt{\frac{1}{4}(\lambda_1 - \lambda_2)^2 + \lambda_4^2}, \\ c_{\pm} &= \frac{1}{2}(\lambda_1 + \lambda_2) \pm \sqrt{\frac{1}{4}(\lambda_1 - \lambda_2)^2 + \lambda_5^2}, \\ e_{\pm} &= \lambda_3 + 2\lambda_4 \pm 3\lambda_5, \\ f_{\pm} &= \lambda_3 \pm \lambda_4, \\ g_{\pm} &= \lambda_3 \pm \lambda_5. \end{aligned} \quad (3.4)$$

The model can give additional contributions to the oblique parameters (S, T, and U) by the exchange of extra Higgs fields in the loop diagram of gauge boson self-energy. We employ the **2HDMC** [66] package to calculate the S, T, and U, and consider the fit results of Ref. [61],

$$S = -0.01 \pm 0.10, \quad T = 0.03 \pm 0.12, \quad U = 0.02 \pm 0.11, \quad (3.5)$$

with the correlation coefficients

$$\rho_{ST} = 0.92, \quad \rho_{SU} = -0.80, \quad \rho_{TU} = -0.93. \quad (3.6)$$

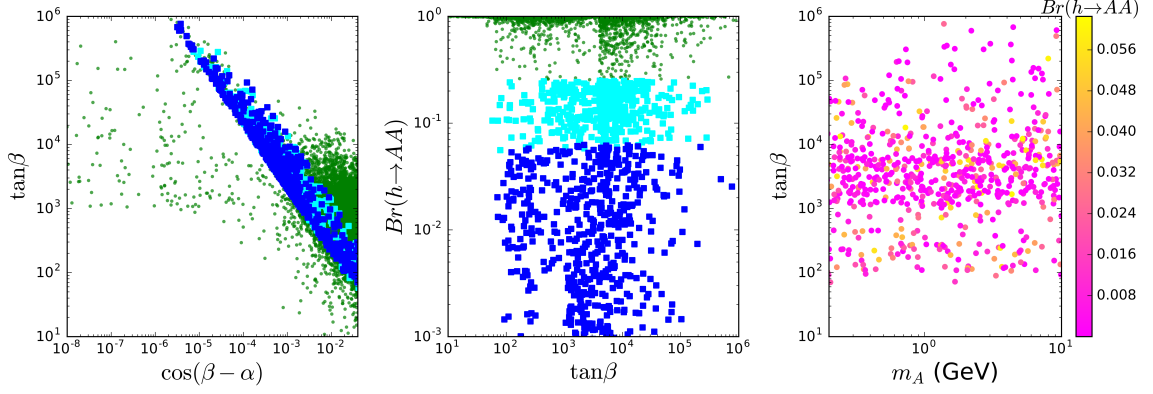


Figure 1. All the samples are allowed by the theoretical constraints and the oblique parameters. The bullets and squares are excluded and allowed by the bound of $Br(h \rightarrow AA) < 0.24$, respectively. For left and middle panels, the light squares (cyan) and the dark squares (blue) are excluded and allowed by the diphoton signal data of the 125 GeV Higgs. The dark squares (blue) in the left and middle panels are projected on the plane of $\tan \beta$ and m_A in the right panel.

In our calculations, $\cos(\beta - \alpha)$, $\tan \beta$, m_H , $m_{H^\pm, H}$, and m_A are scanned over in the following ranges,

$$\begin{aligned} 0 \leq \cos(\beta - \alpha) \leq 0.04, \quad 10 \leq \tan \beta \leq 10^6, \\ 130 \text{ GeV} \leq m_H = m_{H^\pm} \leq 400 \text{ GeV}, \quad 0.2 \text{ GeV} \leq m_A \leq 10 \text{ GeV}, \end{aligned} \quad (3.7)$$

where $m_H = m_{H^\pm}$ is favored by the constraints of the oblique parameters. According to the first expression of Eq. (2.7), the perturbativity requirement of λ_1 favors $m_{12}^2 - m_H^2 s_\beta c_\beta \rightarrow 0$ for a very large $\tan \beta$. However, if $\cos(\beta - \alpha) = 0$ and $\frac{m_{12}^2}{c_\beta s_\beta} = m_H^2$ hold exactly, the last condition of Eq. (3.2) will lead to a strong bound,

$$m_h^2 + m_A^2 > m_H^2, \quad (3.8)$$

which is not satisfied in the chosen parameter space. Therefore, the difference between m_{12}^2 and $m_H^2 s_\beta c_\beta$ need fine-tuning, and the tuning becomes more finely as $\tan \beta$ increases. Hence, we manually take $\tan \beta \leq 10^6$.

After imposing the constraints of theory, the oblique parameters, $Br(h \rightarrow AA) < 0.24$, and the diphoton signal data of the 125 GeV Higgs, we project the surviving samples in Fig. 1. From Fig. 1, we find that the requirement of $Br(h \rightarrow AA) < 0.24$ leads to a strong correlation between $\cos(\beta - \alpha)$ and $\tan \beta$, and excludes much of the parameter space that is consistent with the theoretical constraints. The coupling constant of hAA is

$$g_{hAA} = \frac{2 \cos(\beta - \alpha)}{v t_{2\beta}} \left(m_h^2 - \frac{m_{12}^2}{c_\beta s_\beta} \right) + \frac{\sin(\beta - \alpha)}{v} \left(2m_A^2 + m_h^2 - \frac{2m_{12}^2}{c_\beta s_\beta} \right), \quad (3.9)$$

where the shorthand notations $t_{2\beta} \equiv \tan 2\beta$. For a large $\tan \beta$ and $\cos(\beta - \alpha) \rightarrow 0$, the constraints of theory favor $\frac{m_{12}^2}{c_\beta s_\beta} \rightarrow m_H^2$. Thus, $g_{hAA} \rightarrow 0$ leads to the condition,

$$\cos(\beta - \alpha) \rightarrow \frac{1}{\tan \beta} \frac{2m_A^2 + m_h^2 - 2m_H^2}{m_h^2 - m_H^2}. \quad (3.10)$$

The $h \rightarrow AA$ channel enhances the total width of h , and then decreases the theoretical value of $Br(h \rightarrow \gamma\gamma)$. Therefore, combining the bound of the diphoton signal strength of the 125 GeV Higgs, $Br(h \rightarrow AA) > 0.07$ is excluded, which points to $\tan\beta \gtrsim 10^2$ as can be seen in Fig. 1 left. $Br(h \rightarrow AA)$ does not depend on m_A and $\tan\beta$, as shown in Fig. 1 right. $Br(h \rightarrow AA) > 10^{-2}$ can be obtained almost in the whole interested parameter space, as long as $\tan\beta \gtrsim 10^2$. Hence, in the following discussion of the sensitivity on the parameter space $(m_A, \tan\beta)$, we further restrain it at

$$0.2 \text{ GeV} \leq m_A \leq 10 \text{ GeV}, \text{ and } 10^2 \leq \tan\beta \leq 10^6, \quad (3.11)$$

to satisfy the limits on the $Br(h \rightarrow AA)$. The mass of A is chosen so that it can be long-lived, can be abundantly produced via mediated bosons, and is not excluded by the existing limits mentioned below.

There are existing experimental constraints on a light pseudoscalar: SuperNova [68, 69], searches for axion-like from particles from CHARM [70, 71], B meson decays [72, 73] and D meson decays [74] from LHCb, Kaon decays from NA62 [75], MicroBooNE [76], and E949 [77]. These constraints will be considered in the following discussions.

4 The detection of A as a long-lived particle

Because the couplings of A with the fermions are proportional to $1/\tan\beta$, and a sufficient large $\tan\beta$ can make a light A to be a LLP. Depending on its mass, the decay modes of A include $A \rightarrow \ell^+\ell^-$, $q\bar{q}$, gg , $\gamma\gamma$. The **2HDMC** package is employed to calculate the widths of $A \rightarrow \ell^+\ell^-$, $\gamma\gamma$ for $0.2 \text{ GeV} \leq m_A \leq 10 \text{ GeV}$ and those of $A \rightarrow q\bar{q}$, gg for $3 \text{ GeV} \leq m_A \leq 10 \text{ GeV}$. Below 3 GeV, the partonic description become less reliable, and we take the approaches of Ref. [46, 78, 79] to calculate the hadronic decays of A . The results of the branching ratio of different decay channels of A is shown in Fig. 2 left. For $0.2 \text{ GeV} < m_A \lesssim 3 \text{ GeV}$, A dominantly decay into muons, except the resonance of η and K mesons, where decay to the corresponding mesons becomes substantial. For $m_A \gtrsim 3 \text{ GeV}$, decay into heavy quarks and τ pairs appears and are the leading channels. This is reflected in the total width as shown in Fig. 2 right. As shown, For $0.2 \text{ GeV} < m_A \lesssim 3 \text{ GeV}$, with $\tan\beta \gtrsim 10^4$, the total decay width becomes so small that the decay length becomes larger than order of meters. For $m_A \gtrsim 3 \text{ GeV}$, since the decay into heavy quarks and τ pairs open up, the decay width increases substantially, now $\tan\beta \gtrsim 10^5$ is required to achieve order of meters decay length. And such long-lived A can be captured by the LLP detectors.

The production of A at the LHC is dominantly via the following electroweak processes:

$$pp \rightarrow W^\pm \rightarrow H^\pm A, \quad (4.1)$$

$$pp \rightarrow Z \rightarrow HA, \quad (4.2)$$

$$pp \rightarrow h \rightarrow AA. \quad (4.3)$$

For $m_H = m_{H^\pm} \gg m_A$, $H \rightarrow AZ$ and $H^\pm \rightarrow W^\pm A$ are the dominant decay modes of H , H^\pm . Hence, in the final states of $pp \rightarrow W^\pm/Z \rightarrow H^\pm/HA$ processes, we have $W^\pm/Z + LLP$ signatures. These final states can be constrained by the mono W/Z searches

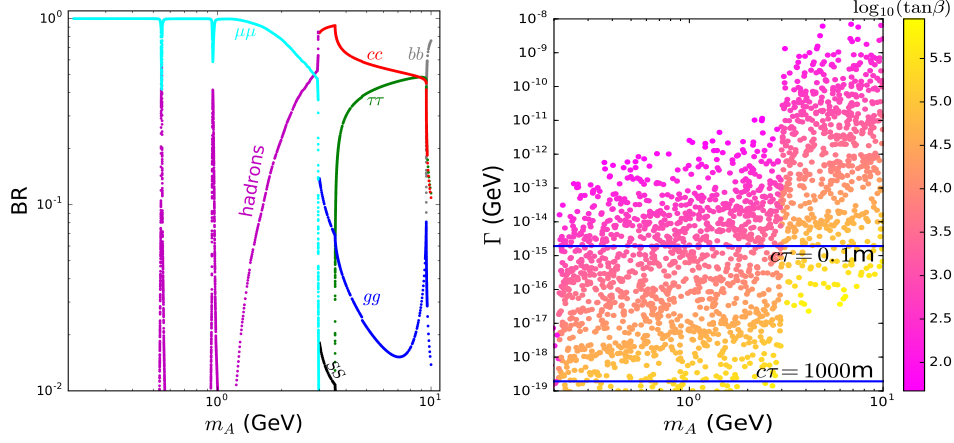


Figure 2. Left: The branching ratio of different decay channels of A . Right: The width of A versus m_A satisfying the constraints of theory [63] and the oblique parameters [61, 66], $Br(h \rightarrow AA) < 0.24$ [58–60], and the diphoton signal data of the 125 GeV Higgs [61].

at the LHC, which limits $\sigma(pp \rightarrow W^\pm/Z \rightarrow H^\pm/HA) \lesssim 1.5$ pb [80]. The cross section only depends on $m_{H^\pm/H}$ and m_A , since $m_{H^\pm/H} \gg m_A$ and coupling of $(W/Z)(H^\pm/H)A$ is $m_{W/Z}/(2v)$ for $|\sin(\beta - \alpha)| \rightarrow 1$. In Fig. 3, we show $\sigma(pp \rightarrow W^\pm/Z \rightarrow H^\pm/HA)$ as a function of $m_{H^\pm/H}$, fixing $m_A = 1$ GeV, at 14 TeV LHC. As $m_{H^\pm/H}$ increases, the phase space becomes smaller, so the cross section decrease rapidly from ≈ 1.5 pb at $m_{H^\pm/H} = 130$ GeV, to ≈ 22 fb at $m_{H^\pm/H} \approx 400$ GeV. Hence, within $130 \text{ GeV} < m_{H^\pm/H} < 400 \text{ GeV}$, the current limits on mono W/Z searches can be satisfied.

So we take two benchmark scenarios to reflect the dependence on $m_{H^\pm/H}$,

$$m_{H^\pm/H} = 130 \text{ GeV}, \sigma(pp \rightarrow W^\pm/Z \rightarrow H^\pm/HA) \approx 1.5 \text{ pb}. \quad (4.4)$$

$$m_{H^\pm/H} = 400 \text{ GeV}, \sigma(pp \rightarrow W^\pm/Z \rightarrow H^\pm/HA) \approx 22 \text{ fb}. \quad (4.5)$$

The production of the A at the LHC is sufficient large enough to allow for possible detection at the LLP detectors including FASER, FACET, MAPP and MATHUSLA. Assuming the acceptance of the LLPs at these detectors is 100%, the expected signal events N_S are controlled by the probability of the A s in the final states to enter the volume of the respected detectors, such as

$$N_S = \mathcal{L}_{\text{int}} \int dp d\theta \frac{d\sigma}{dp d\theta} P(p, \theta, c\tau), \quad (4.6)$$

where p, θ and $c\tau$ are the three-momentum, angle between the beam line with the decay location, and proper decay length of the A s in the final states.

To estimate the probability, the geometry and location of the LLP detectors is needed. We summarise the necessary information of these detectors in the following.

FASER is placed at the very forward direction with $\theta \lesssim 10^{-3}$, and around 480 meters away from the ATLAS IP. It is already installed and collecting data since the Run 3 of the LHC, and the first phase of its setup is aiming to accumulating 150 fb^{-1} integrated luminosity [3, 4]. Since A in the final states are not likely to fly in such forward direction,

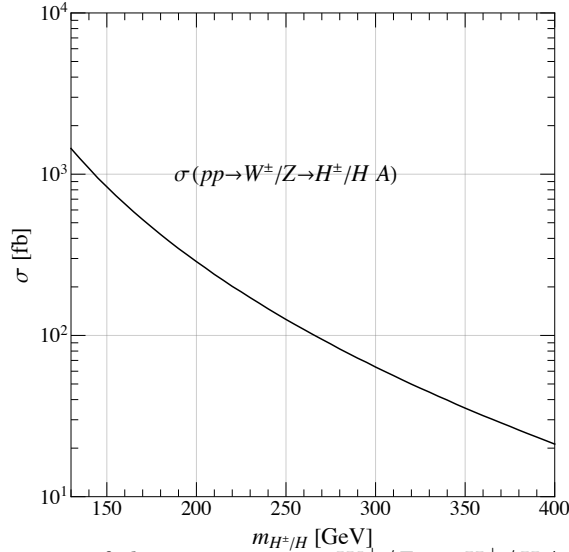


Figure 3. Left: Cross section of the process $pp \rightarrow W^\pm/Z \rightarrow H^\pm/HA$ as a function of $m_{H^\pm/H}$. We fix $m_{H^\pm} = m_H$, and $m_A = 1$ GeV.

we do not expect the FASER to yield positive results for our considered signals, even with its second phase setup, FASER-2 at the HL-LHC with 3000 fb^{-1} integrated luminosity. Nevertheless, we still list the relevant information of the FASER-2

$$L_{xy} < 1 \text{ m}, \quad 475 \text{ m} < L_z < 480 \text{ m}, \quad \mathcal{L} = 3000 \text{ fb}^{-1}, \quad (4.7)$$

and calculate the signal events in the following procedures.

FACET is a LLP detector, recently proposed to be installed around 100 meters away from the CMS IP [5]. Like FASER, it is a cylinder, symmetrical around the beam line in a very forward direction, but with larger solid angle coverage, $2 \times 10^{-3} \lesssim \theta \lesssim 5 \times 10^{-3}$, since it is closer to the IP, such as

$$0.18 \text{ m} < L_{xy} < 0.5 \text{ m}, \quad 101 \text{ m} < L_z < 119 \text{ m}, \quad \mathcal{L} = 3000 \text{ fb}^{-1}. \quad (4.8)$$

MAPP is a new sub-detector of the MoEDAL detector, aiming for searching LLPs [6, 7]. Unlike the FASER and FACET detectors, it is a box, which is not symmetrical around the beam line, located around 50 meters away from the LHCb IP. There are two phase setup of the MAPP detectors, in which the first setup is already installed and collecting data since Run 3 of the LHC. Nevertheless, we only take the second phase setup of the MAPP at the HL-LHC, MAPP-2 into account to get the optimistic results. To simplify the calculation, we take the shape of the MAPP-2 as an ideal box,

$$3 \text{ m} \lesssim L_x \lesssim 19 \text{ m}, \quad -2 \text{ m} < L_y < 1 \text{ m}, \quad -61 \text{ m} \lesssim L_z \lesssim -29 \text{ m}, \quad \mathcal{L} = 300 \text{ fb}^{-1}, \quad (4.9)$$

while the realistic information of the MAPP-2 can be found in Ref. [41]

MATHUSLA is a large surface detector on the ground of the ATLAS IP [8]. Unlike the aforementioned detectors, it is placed at the transverse direction, with the largest solid angle coverage, proposed to be installed at the HL-LHC era,

$$-100 \text{ m} < L_x < 100 \text{ m}, \quad 100 \text{ m} < L_y < 120 \text{ m}, \quad 100 \text{ m} < L_z < 300 \text{ m}, \quad \mathcal{L} = 3000 \text{ fb}^{-1}. \quad (4.10)$$

Although the installation of the MATHUSLA is still in discussion, we take it as an example to show the most positive outcome of the LLP detectors.

For the four detectors, given whether they are symmetrical around the beam line, we use two strategies to estimate the probability of the A entering into the detector volume. FASER and FACET have cylindrical symmetry around the beam line, hence

$$P(p, \theta, c\tau) = \left(e^{-(L-\Delta)/d} - e^{-L/d} \right) \Theta(R - \tan \theta L) \approx \frac{\Delta}{d} e^{-L/d} \Theta(R - \theta L) \quad (4.11)$$

where Θ is the Heaviside function, p is the three momentum of A , $d = c\tau p/m_A$ is the decay length of A in the lab frame, θ is the angle of the momentum of A to the beam line, L is the farthest longitudinal distance to the IP of the detector, Δ is the longitudinal length of the detector, and R is the radius in the xoy plane, respectively.

The differential cross section $\frac{d\sigma}{dpd\theta}$ needs to be simulated via Monte-Carlo methods. The processes are generated after feeding the Universal FeynRules Output (UFO) [81, 82] to the event generator **MadGraph5aMC@NLO** v3.5.1 [83]. After that, the differential cross section is obtained by the event generator, whereas the effects of shower, hadronization, etc are handled by **PYTHIA** v8.306 [84].

Nonetheless, MAPP and MATHUSLA do not possess cylindrical symmetry, and the probability in such detectors are not analytical. Hence, we use full Monte-Carlo methods, as we further use inverse sampling methods to simulate the exponential distribution of the lab decay length of the A .

To graphically illustrate $P(p, \theta, c\tau)$ for different detectors and processes, we show the (d, θ) distribution of A from the processes $pp \rightarrow W^\pm/Z \rightarrow H^\pm/HA$ (left), and $pp \rightarrow h \rightarrow AA$ (right) at the 14 TeV LHC, in Fig. 4. We fix $m_A = 1 \text{ GeV}$, $\tan \beta = 10^4$ so $c\tau \approx 0.8 \text{ m}$. The masses of heavy and charged Higgs is fixed as $m_{H^\pm/H} = 130 \text{ GeV}$. From the figure, it is clear that A via mediated bosons are close to the transverse direction, where MAPP and MATHUSLA has large coverage, while FACET and FASER can only get the tail of the distribution. Therefore, we expect better sensitivity at MAPP and MATHUSLA.

Following the above procedures, we estimate the sensitivity to the $\tan \beta$ at the FASER-2, FACET, MAPP-2 and MATHUSLA. The 95% confidence level (CL) sensitivity is set by requiring $N_S \gtrsim 3$. Although we set our interested parameter space in Eq. 3.11 with $\tan \beta < 10^6$, we extend it to $\tan \beta < 10^8$ as the LLP detectors might be sensitive to. Nevertheless, such values of $\tan \beta$ requires over fine-tuning, so we put the line labelled ‘theory’ to reflect that ¹.

We begin with the process $pp \rightarrow W^\pm/Z \rightarrow H^\pm/HA$ with $m_{H^\pm/H} = 130 \text{ GeV}$, as the results are shown in Fig. 5. The current limits from CHARM [70, 71], LHCb [72–74], NA62 [75] is overlaid for comparison. The CHARM experiments can already probe

¹Such $\tan \beta \gtrsim 10^6$ requires $|m_{12}^2 - m_H^2 s_\beta c_\beta| \lesssim 10^{-14}$, which is over fine-tuned.

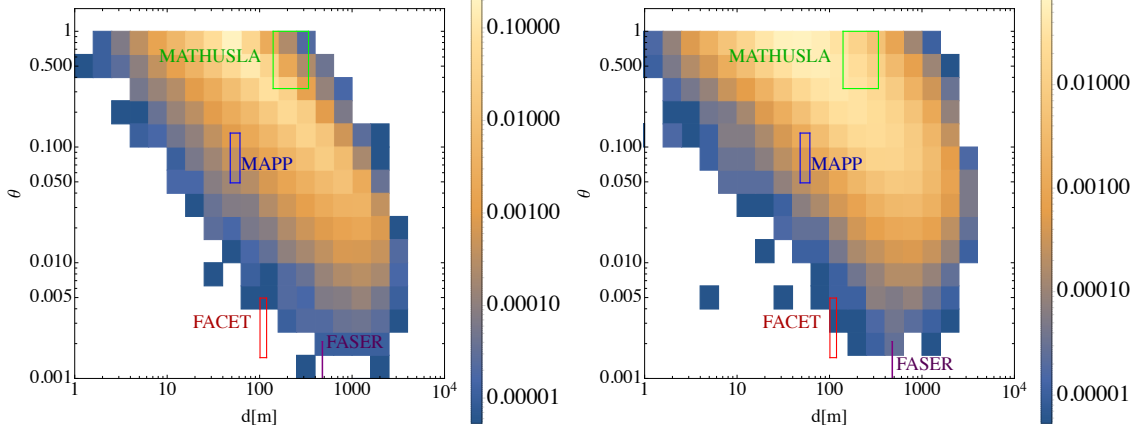


Figure 4. (d, θ) distribution of A from the processes $pp \rightarrow W^\pm/Z \rightarrow H^\pm/HA$ (left), and $pp \rightarrow h \rightarrow AA$ (right) at the 14 TeV LHC. $d = c\tau p/m_A$ is the decay length of A in the lab frame, and θ is the angle of the momentum of A to the beam line. The probability distribution function is illustrated by the color. The geometrical coverage of FASER-2, FACET, MAPP-2 and MATHUSLA is overlaid. We fix $m_A = 1$ GeV $\tan \beta = 10^4$ so $c\tau \approx 0.8$ m. The masses of heavy and charged Higgs is fixed as $m_{H^\pm/H} = 130$ GeV.

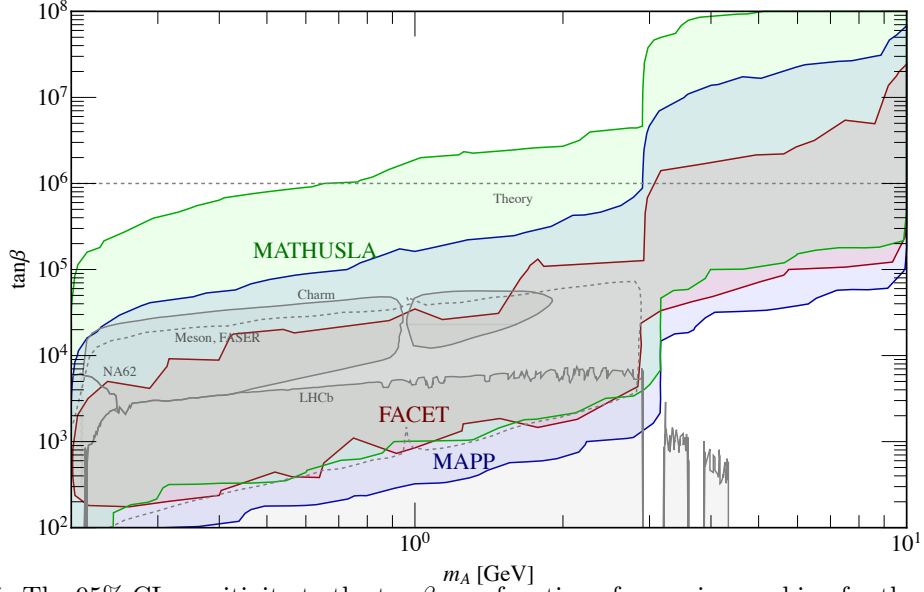


Figure 5. The 95% CL sensitivity to the $\tan \beta$ as a function of m_A , via searching for the long-lived particle signature of the $pp \rightarrow W^\pm/Z \rightarrow H^\pm/HA$ at FACET, MAPP-2 and MATHUSLA. The current limits from CHARM [70, 71], LHCb [72–74], NA62 [75] is overlaid for comparison. The gray curve is the expected sensitivity from searching A from meson decay at FASER-2 [46]. The line ‘theory’ is put at $\tan \beta \leq 10^6$, reflects where the value of $\tan \beta$ requires over fine-tuning. We fix $m_{H^\pm/H} = 130$ GeV.

$\tan \beta \sim 5 \times 10^4$ for $m_A \lesssim 2$ GeV, where A is long-lived. Under that, via searching for the anomalous decays of various mesons, LHCb and NA62 can probe $\tan \beta \lesssim 4 \times 10^3$ in $m_A \lesssim 3$ GeV. Hence, there exists a valley between the three experiments, which can be filled by

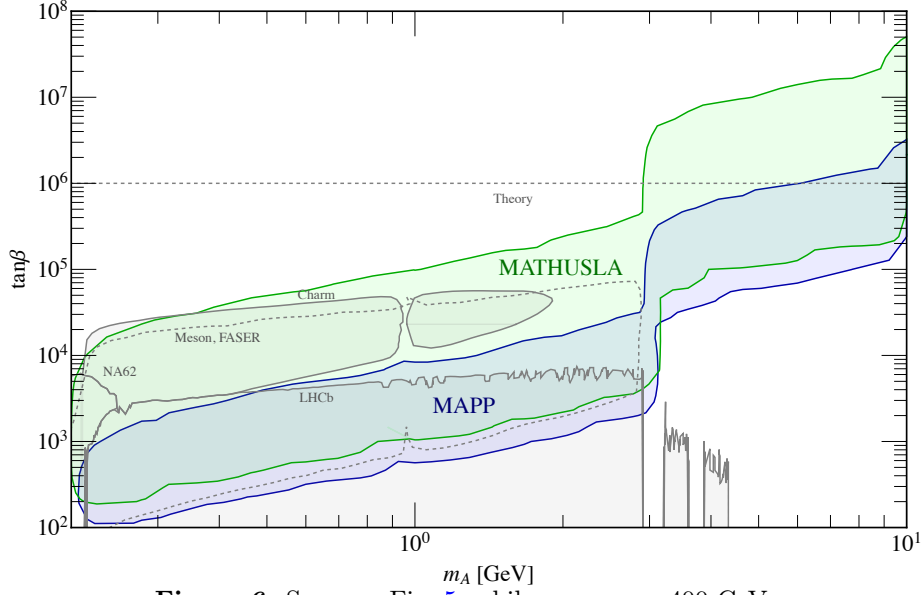


Figure 6. Same as Fig. 5, while $m_{H^\pm/H} = 400$ GeV.

searching for the long-lived A from the meson decays at FASER and FASER-2 [46].

Nevertheless, for our processes, $pp \rightarrow W^\pm/Z \rightarrow H^\pm/HA$, the A in the final states are not likely to be distributed in such very forward direction where FASER is located as indicated by Fig. 4. Subsequently, as expected, there is no sensitivity at either FASER or FASER-2. On the other hand, since FACET has larger solid angle coverage, it yields positive results. Although FACET is located 100 meters away, A is so light that it is boosted by $\mathcal{O}(10)$ times, so the sensitivity contour roughly follows the distribution of the decay length $c\tau \sim 1$ m, as shown in Fig. 2. For $m_A < 3$ GeV, FACET can touch $\tan\beta \lesssim 5 \times 10^4$, which is already ruled out by either the CHARM or meson decays at the FASER. Aiming at $m_A \gtrsim 3$ GeV, multiple channels for A to decay into mesons open up, such that the required $\tan\beta$ to make A long-lived suddenly jumps. In such mass range, A cannot be generated by light meson decays, so there rarely exist any current limits, only the heavy meson decays at the LHCb giving rather softer constraints. Nevertheless, such heavy A can still be produced via mediated weak boson, and we can probe $\tan\beta \lesssim 10^{6-7}$ at FACET, which is not explored yet.

Although MAPP-2 is placed only half distant away comparing to FACET, due to its much larger solid angle coverage, up to $\theta \lesssim 0.1$, it has shown better sensitivity, extends roughly half magnitude more both at lower and higher edge of $\tan\beta$ in a very similar mass range of A . The situation becomes even better for MATHUSLA, with large coverage in angle (up to $\theta \lesssim 1$), and so in distance, it can probe $\tan\beta \lesssim 10^{6-7}$ for $m_A < 3$ GeV, and $\tan\beta \lesssim 10^8$ for $3 \text{ GeV} < m_A < 10 \text{ GeV}$, surpassing the current limits by at least one magnitude.

It is interesting to discuss the dependence of the sensitivity on different $m_{H^\pm/H}$. In Fig. 6, we show the sensitivity from the same processes, while the mass of H^\pm/H is larger, $m_{H^\pm/H} = 400$ GeV. As indicated in Fig. 3 left, the cross section of $\sigma(pp \rightarrow W^\pm/Z \rightarrow$

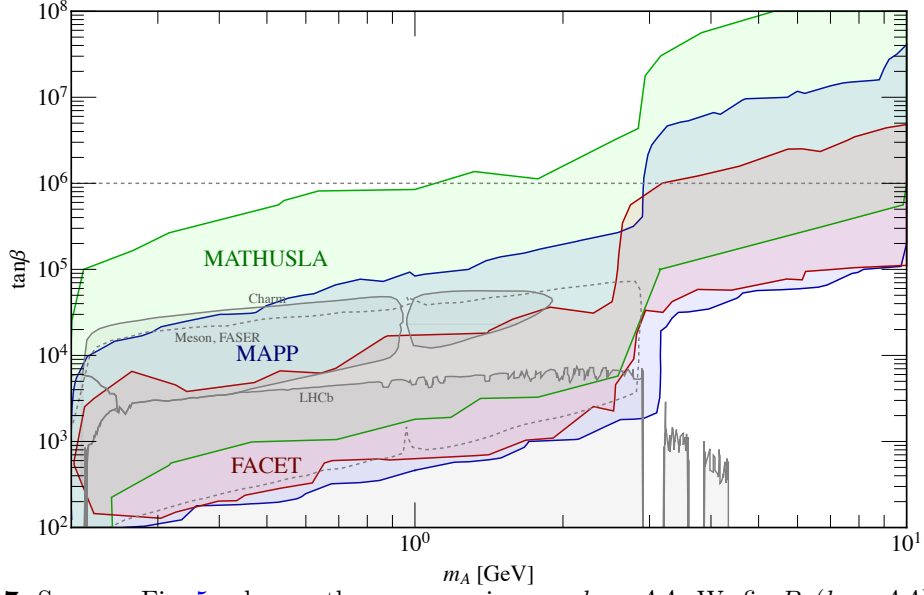


Figure 7. Same as Fig. 5, whereas the processes is $pp \rightarrow h \rightarrow AA$. We fix $Br(h \rightarrow AA) = 0.01$.

H^\pm/HA) becomes about one hundred times smaller, so the sensitivity is expected to be reduced. For this benchmark, FACET no longer cover any parameter space at all, due to its low angular coverage. The sensitivity of MAPP shrinks, only extends to $\tan \beta \lesssim 10^{3-4}$ for $m_A \lesssim 3$ GeV, still comparable to the current limits from LHCb. Nevertheless, for $m_A \lesssim 2$ GeV, its sensitivity is worse than the ones of CHARM for at least half magnitude. When $m_A \gtrsim 3$ GeV, MAPP reaches $\tan \beta \lesssim 10^6$, much exceeds the current limits at LHCb. When it comes to MATHUSLA, due to its large geometrical coverage, the sensitivity is still better than the current limits at CHARM, and probes new region where $\tan \beta \lesssim 10^7$ for $m_A \gtrsim 3$ GeV.

As shown in Fig. 3 left, $\sigma(pp \rightarrow W^\pm/Z \rightarrow H^\pm/HA)$ decreases as $m_{H^\pm/H}$ becomes larger. So the benchmark $m_{H^\pm/H} = 400$ GeV is serving to show the worst sensitivity for $130 \text{ GeV} < m_{H^\pm/H} < 400$ GeV. Since we have shown that with $m_{H^\pm/H} = 400$ GeV, MATHUSLA and MAPP is able to obtain comparable sensitivity for $m_A \lesssim 3$ GeV to the current limits, and explores new parameter space for $m_A \gtrsim 3$ GeV, thus we can conclude that for the whole parameter space of $130 \text{ GeV} < m_{H^\pm/H} < 400$ GeV, we are expecting better sensitivity on $(m_A, \tan \beta)$ at LLP detectors than the current limits from the processes $\sigma(pp \rightarrow W^\pm/Z \rightarrow H^\pm/HA)$.

A can also be pair-produced from the decay of the SM Higgs. In Fig. 1, we have shown that $Br(h \rightarrow AA) = 0.01$ can be obtained in a very broad parameter space. At 14 TeV LHC, we have the full SM Higgs production, $\sigma(pp \rightarrow h) \approx 56 \text{ pb}$ [85], hence $\sigma(pp \rightarrow h \rightarrow AA)$ can reach $\approx 5.6 \text{ pb}$, which is at least more than 3 times larger than $\sigma(pp \rightarrow W^\pm/Z \rightarrow H^\pm/HA)$. Regarded as an optimistic prospects, we fix $Br(h \rightarrow AA) = 0.01$ and show the sensitivity from LLP searches of this process in Fig. 7. The final states of the SM Higgs decays is more likely to distribute at the transverse direction, which FASER can not cover, and the sensitivity of FACET becomes worse comparing to the case where $m_{H^\pm/H} = 130$ GeV

for the processes $pp \rightarrow W^\pm/Z \rightarrow H^\pm/HA$. MAPP and MATHUSLA are closer to the transverse direction, so still yield similar sensitivity, strongly surpass the current limits.

5 Conclusion

In this work, we have explored the possibility to probe the type-I 2HDM model via searching for the LLP final states of the light Higgs A , at FASER-2, FACET, MAPP-2 and MATHUSLA, directly produced via mediated bosons including $pp \rightarrow W^\pm/Z \rightarrow H^\pm/HA$ and $pp \rightarrow h \rightarrow AA$. LLPs from such processes can be distributed at the transverse direction, rather than the forward direction where FASER located, hence we expect better sensitivity at MAPP-2 and MATHUSLA.

We have focused on light A with masses up to 10 GeV. The decay length of A , is only dependent on its masses and the ratio between the vevs of the two Higgs doublets, $\tan\beta$. When $\tan\beta$ is sufficiently large, A can have decay length $\mathcal{O}(\text{m})$, resulting unique signatures as LLPs at the LHC. Such LLP signatures can be smoking-gun of the physics beyond the SM, as the SM background is nearly zero. Targetting at such signatures, multiple LLP detectors are proposed. Among them, FASER and MAPP are already installed and collecting data since run 3 of the LHC.

We have discussed the sensitivity reach of these detectors from the $pp \rightarrow W^\pm/Z \rightarrow H^\pm/HA$ processes. As the cross section also dependent on m_{H^\pm} and m_H , we take two benchmarks where $m_{H^\pm} = m_H = 130$ and 400 GeV, respectively. The sensitivity on the parameter space $(m_A, \tan\beta)$ is obtained and compared to the current limits mainly from CHARM and LHCb, as well as the projected limits of searching for A from meson decays at FASER-2 in Ref. [46]. We have shown that, since the final states from direct production are not likely to distributed in such forward direction where FASER located, it has no sensitivity at all. Anyway, other LLP detectors, especially MATHUSLA, have shown at least comparable sensitivity to the current limits for $m_A \lesssim 3$ GeV, with $\tan\beta \lesssim 10^5$, and extends the sensitivity for $m_A \gtrsim 3$ GeV with $\tan\beta \lesssim 10^{7-8}$ where have never been probed. Giving that $\sigma(pp \rightarrow W^\pm/Z \rightarrow H^\pm/HA)$ decreases as $m_{H^\pm/H}$ increases, we can expect the same conclusion within the range $130 \text{ GeV} < m_H^\pm = m_H < 400 \text{ GeV}$.

The sensitivity from the channels of the SM Higgs decays, $pp \rightarrow h \rightarrow AA$ is also shown. Giving that $Br(h \rightarrow AA)$ is independent of both m_A and $\tan\beta$, we fix it at $Br(h \rightarrow AA) = 0.01$. For such channels, A in the final states are situated at directions closer to the transverse ones, hence FASER-2 fail to show any sensitivity, and the sensitivity of FACET shrinks. Anyway, MAPP-2 and MATHUSLA can still show comparable sensitivity just as the case of $pp \rightarrow W^\pm/Z \rightarrow H^\pm/HA$ when $m_H^\pm = m_H = 130 \text{ GeV}$.

Acknowledgments

This work was supported by the National Natural Science Foundation of China under grants No.12205153, 11975013, 11805001, the Natural Science Foundation of Shandong province ZR2023MA038, and the Fundamental Research Funds for the Central Universities under Grant No.JZ2023HG TB0222.

References

- [1] ATLAS collaboration, G. Aad et al., *Observation of a new particle in the search for the Standard Model Higgs boson with the ATLAS detector at the LHC*, *Phys. Lett. B* **716** (2012) 1–29, [[1207.7214](#)].
- [2] CMS collaboration, S. Chatrchyan et al., *Observation of a New Boson at a Mass of 125 GeV with the CMS Experiment at the LHC*, *Phys. Lett. B* **716** (2012) 30–61, [[1207.7235](#)].
- [3] FASER collaboration, B. Petersen, *First Physics Results from the FASER Experiment*, in *57th Rencontres de Moriond on Electroweak Interactions and Unified Theories*, 5, 2023. [2305.08665](#).
- [4] FASER collaboration, H. Abreu et al., *Search for dark photons with the FASER detector at the LHC*, *Phys. Lett. B* **848** (2024) 138378, [[2308.05587](#)].
- [5] S. Cerci et al., *FACET: A new long-lived particle detector in the very forward region of the CMS experiment*, *JHEP* **06** (2022) 110, [[2201.00019](#)].
- [6] J. L. Pinfold, *The MoEDAL Experiment at the LHC—A Progress Report*, *Universe* **5** (2019) 47.
- [7] MoEDAL-MAPP collaboration, B. Acharya et al., *MoEDAL-MAPP, an LHC Dedicated Detector Search Facility*, in *Snowmass 2021*, 9, 2022. [2209.03988](#).
- [8] J. P. Chou, D. Curtin and H. J. Lubatti, *New Detectors to Explore the Lifetime Frontier*, *Phys. Lett. B* **767** (2017) 29–36, [[1606.06298](#)].
- [9] M. Bauer, O. Brandt, L. Lee and C. Ohm, *ANUBIS: Proposal to search for long-lived neutral particles in CERN service shafts*, [1909.13022](#).
- [10] V. V. Gligorov, S. Knapen, M. Papucci and D. J. Robinson, *Searching for Long-lived Particles: A Compact Detector for Exotics at LHCb*, *Phys. Rev. D* **97** (2018) 015023, [[1708.09395](#)].
- [11] V. V. Gligorov, S. Knapen, B. Nachman, M. Papucci and D. J. Robinson, *Leveraging the ALICE/L3 cavern for long-lived particle searches*, *Phys. Rev. D* **99** (2019) 015023, [[1810.03636](#)].
- [12] D. Tucker-Smith and N. Weiner, *Inelastic dark matter*, *Phys. Rev. D* **64** (2001) 043502, [[hep-ph/0101138](#)].
- [13] K. R. Dienes and B. Thomas, *Dynamical Dark Matter: I. Theoretical Overview*, *Phys. Rev. D* **85** (2012) 083523, [[1106.4546](#)].
- [14] K. R. Dienes and B. Thomas, *Dynamical Dark Matter: II. An Explicit Model*, *Phys. Rev. D* **85** (2012) 083524, [[1107.0721](#)].
- [15] K. R. Dienes and B. Thomas, *Phenomenological Constraints on Axion Models of Dynamical Dark Matter*, *Phys. Rev. D* **86** (2012) 055013, [[1203.1923](#)].
- [16] Y. Hochberg, E. Kuflik and H. Murayama, *SIMP Spectroscopy*, *JHEP* **05** (2016) 090, [[1512.07917](#)].
- [17] M. J. Strassler and K. M. Zurek, *Echoes of a hidden valley at hadron colliders*, *Phys. Lett. B* **651** (2007) 374–379, [[hep-ph/0604261](#)].
- [18] M. J. Strassler and K. M. Zurek, *Discovering the Higgs through highly-displaced vertices*, *Phys. Lett. B* **661** (2008) 263–267, [[hep-ph/0605193](#)].

- [19] B. Holdom, *Two $U(1)$'s and Epsilon Charge Shifts*, *Phys. Lett. B* **166** (1986) 196–198.
- [20] M. Bauer, P. Foldenauer and J. Jaeckel, *Hunting All the Hidden Photons*, *JHEP* **07** (2018) 094, [[1803.05466](#)].
- [21] M. Fabbrichesi, E. Gabrielli and G. Lanfranchi, *The Dark Photon*, [2005.01515](#).
- [22] A. Caputo, A. J. Millar, C. A. J. O'Hare and E. Vitagliano, *Dark photon limits: A handbook*, *Phys. Rev. D* **104** (2021) 095029, [[2105.04565](#)].
- [23] R. D. Peccei and H. R. Quinn, *CP Conservation in the Presence of Instantons*, *Phys. Rev. Lett.* **38** (1977) 1440–1443.
- [24] R. D. Peccei and H. R. Quinn, *Constraints Imposed by CP Conservation in the Presence of Instantons*, *Phys. Rev. D* **16** (1977) 1791–1797.
- [25] J. Jaeckel and A. Ringwald, *The Low-Energy Frontier of Particle Physics*, *Ann. Rev. Nucl. Part. Sci.* **60** (2010) 405–437, [[1002.0329](#)].
- [26] M. Bauer, M. Neubert and A. Thamm, *Collider Probes of Axion-Like Particles*, *JHEP* **12** (2017) 044, [[1708.00443](#)].
- [27] M. Gell-Mann, P. Ramond and R. Slansky, *Complex Spinors and Unified Theories*, *Conf. Proc. C* **790927** (1979) 315–321, [[1306.4669](#)].
- [28] R. N. Mohapatra and G. Senjanovic, *Neutrino Mass and Spontaneous Parity Nonconservation*, *Phys. Rev. Lett.* **44** (1980) 912.
- [29] J. Schechter and J. W. F. Valle, *Neutrino Masses in $SU(2) \times U(1)$ Theories*, *Phys. Rev. D* **22** (1980) 2227.
- [30] T. Asaka and M. Shaposhnikov, *The ν MSM, dark matter and baryon asymmetry of the universe*, *Phys. Lett. B* **620** (2005) 17–26, [[hep-ph/0505013](#)].
- [31] J. Kersten and A. Y. Smirnov, *Right-Handed Neutrinos at CERN LHC and the Mechanism of Neutrino Mass Generation*, *Phys. Rev. D* **76** (2007) 073005, [[0705.3221](#)].
- [32] M. Drewes and B. Garbrecht, *Combining experimental and cosmological constraints on heavy neutrinos*, *Nucl. Phys. B* **921** (2017) 250–315, [[1502.00477](#)].
- [33] F. F. Deppisch, W. Liu and M. Mitra, *Long-lived Heavy Neutrinos from Higgs Decays*, *JHEP* **08** (2018) 181, [[1804.04075](#)].
- [34] S. Amrith, J. M. Butterworth, F. F. Deppisch, W. Liu, A. Varma and D. Yallup, *LHC Constraints on a $B - L$ Gauge Model using Contur*, *JHEP* **05** (2019) 154, [[1811.11452](#)].
- [35] F. Deppisch, S. Kulkarni and W. Liu, *Heavy neutrino production via Z' at the lifetime frontier*, *Phys. Rev. D* **100** (2019) 035005, [[1905.11889](#)].
- [36] W. Liu, S. Kulkarni and F. F. Deppisch, *Heavy neutrinos at the FCC-hh in the $U(1)_{B-L}$ model*, *Phys. Rev. D* **105** (2022) 095043, [[2202.07310](#)].
- [37] W. Liu, J. Li, J. Li and H. Sun, *Testing the seesaw mechanisms via displaced right-handed neutrinos from a light scalar at the HL-LHC*, *Phys. Rev. D* **106** (2022) 015019, [[2204.03819](#)].
- [38] W. Liu and Y. Zhang, *Testing neutrino dipole portal by long-lived particle detectors at the LHC*, *Eur. Phys. J. C* **83** (2023) 568, [[2302.02081](#)].
- [39] Y. Zhang and W. Liu, *Probing active-sterile neutrino transition magnetic moments at LEP and CEPC*, *Phys. Rev. D* **107** (2023) 095031, [[2301.06050](#)].

- [40] D. Barducci, W. Liu, A. Titov, Z. S. Wang and Y. Zhang, *Probing the dipole portal to heavy neutral leptons via meson decays at the high-luminosity LHC*, *Phys. Rev. D* **108** (2023) 115009, [[2308.16608](#)].
- [41] F. F. Deppisch, S. Kulkarni and W. Liu, *Sterile Neutrinos at MAPP in the B-L Model*, 11, 2023. [2311.01719](#).
- [42] J. Li, W. Liu and H. Sun, *Z' Mediated right-handed Neutrinos from Meson Decays at the FASER*, [2309.05020](#).
- [43] W. Liu and F. F. Deppisch, *Testing Leptogenesis and Seesaw using Long-lived Particle Searches in the B – L Model*, [2312.11165](#).
- [44] P. Bandyopadhyay, M. Frank, S. Parashar and C. Sen, *Interplay of inert doublet and vector-like lepton triplet with displaced vertices at the LHC/FCC and MATHUSLA*, *JHEP* **03** (2024) 109, [[2310.08883](#)].
- [45] Q.-H. Cao, J. Guo, J. Liu, Y. Luo and X.-P. Wang, *Long-lived Searches of Vector-like Lepton and Its Accompanying Scalar at Colliders*, [2311.12934](#).
- [46] F. Kling, S. Li, H. Song, S. Su and W. Su, *Light Scalars at FASER*, *JHEP* **08** (2023) 001, [[2212.06186](#)].
- [47] W. Liu, A. Yang and H. Sun, *Shedding light on the electroweak phase transition from exotic Higgs boson decays at the lifetime frontiers*, *Phys. Rev. D* **105** (2022) 115040, [[2205.08205](#)].
- [48] U. Haisch and L. Schnell, *Long-lived particle phenomenology in the 2HDM+a model*, *JHEP* **04** (2023) 134, [[2302.02735](#)].
- [49] T. D. Lee, *A Theory of Spontaneous T Violation*, *Phys. Rev. D* **8** (1973) 1226–1239.
- [50] H. E. Haber, G. L. Kane and T. Sterling, *The Fermion Mass Scale and Possible Effects of Higgs Bosons on Experimental Observables*, *Nucl. Phys. B* **161** (1979) 493–532.
- [51] L. J. Hall and M. B. Wise, *FLAVOR CHANGING HIGGS - BOSON COUPLINGS*, *Nucl. Phys. B* **187** (1981) 397–408.
- [52] J. F. Donoghue and L. F. Li, *Properties of Charged Higgs Bosons*, *Phys. Rev. D* **19** (1979) 945.
- [53] V. D. Barger, J. L. Hewett and R. J. N. Phillips, *New Constraints on the Charged Higgs Sector in Two Higgs Doublet Models*, *Phys. Rev. D* **41** (1990) 3421–3441.
- [54] Y. Grossman, *Phenomenology of models with more than two Higgs doublets*, *Nucl. Phys. B* **426** (1994) 355–384, [[hep-ph/9401311](#)].
- [55] A. G. Akeroyd and W. J. Stirling, *Light charged Higgs scalars at high-energy e^+e^- colliders*, *Nucl. Phys. B* **447** (1995) 3–17.
- [56] A. G. Akeroyd, *Nonminimal neutral Higgs bosons at LEP-2*, *Phys. Lett. B* **377** (1996) 95–101, [[hep-ph/9603445](#)].
- [57] J. Alimena et al., *Searching for long-lived particles beyond the Standard Model at the Large Hadron Collider*, *J. Phys. G* **47** (2020) 090501, [[1903.04497](#)].
- [58] CMS collaboration, V. Khachatryan et al., *Searches for invisible decays of the Higgs boson in pp collisions at $\sqrt{s} = 7, 8$, and 13 TeV*, *JHEP* **02** (2017) 135, [[1610.09218](#)].
- [59] ATLAS collaboration, G. Aad et al., *Search for invisible decays of a Higgs boson using*

- vector-boson fusion in pp collisions at $\sqrt{s} = 8$ TeV with the ATLAS detector, *JHEP* **01** (2016) 172, [[1508.07869](#)].
- [60] ATLAS collaboration, M. Aaboud et al., *Search for an invisibly decaying Higgs boson or dark matter candidates produced in association with a Z boson in pp collisions at $\sqrt{s} = 13$ TeV with the ATLAS detector*, *Phys. Lett. B* **776** (2018) 318–337, [[1708.09624](#)].
 - [61] PARTICLE DATA GROUP collaboration, P. A. Zyla et al., *Review of Particle Physics*, *PTEP* **2020** (2020) 083C01.
 - [62] L. Wang and X.-F. Han, *Status of the aligned two-Higgs-doublet model confronted with the Higgs data*, *JHEP* **04** (2014) 128, [[1312.4759](#)].
 - [63] N. G. Deshpande and E. Ma, *Pattern of Symmetry Breaking with Two Higgs Doublets*, *Phys. Rev. D* **18** (1978) 2574.
 - [64] S. Kanemura, T. Kubota and E. Takasugi, *Lee-Quigg-Thacker bounds for Higgs boson masses in a two doublet model*, *Phys. Lett. B* **313** (1993) 155–160, [[hep-ph/9303263](#)].
 - [65] A. G. Akeroyd, A. Arhrib and E.-M. Naimi, *Note on tree level unitarity in the general two Higgs doublet model*, *Phys. Lett. B* **490** (2000) 119–124, [[hep-ph/0006035](#)].
 - [66] D. Eriksson, J. Rathsmann and O. Stal, *2HDMC: Two-Higgs-Doublet Model Calculator Physics and Manual*, *Comput. Phys. Commun.* **181** (2010) 189–205, [[0902.0851](#)].
 - [67] L. Wang, *Inflation, electroweak phase transition, and Higgs searches at the LHC in the two-Higgs-doublet model*, *JHEP* **07** (2022) 055, [[2105.02143](#)].
 - [68] M. S. Turner, *Axions from SN 1987a*, *Phys. Rev. Lett.* **60** (1988) 1797.
 - [69] J. R. Ellis and K. A. Olive, *Constraints on Light Particles From Supernova Sn1987a*, *Phys. Lett. B* **193** (1987) 525.
 - [70] CHARM collaboration, F. Bergsma et al., *Search for Axion Like Particle Production in 400-GeV Proton - Copper Interactions*, *Phys. Lett. B* **157** (1985) 458–462.
 - [71] D. Gorbunov, I. Krasnov and S. Suvorov, *Constraints on light scalars from PS191 results*, *Phys. Lett. B* **820** (2021) 136524, [[2105.11102](#)].
 - [72] LHCb collaboration, R. Aaij et al., *Search for hidden-sector bosons in $B^0 \rightarrow K^{*0} \mu^+ \mu^-$ decays*, *Phys. Rev. Lett.* **115** (2015) 161802, [[1508.04094](#)].
 - [73] LHCb collaboration, R. Aaij et al., *Search for long-lived scalar particles in $B^+ \rightarrow K^+ \chi(\mu^+ \mu^-)$ decays*, *Phys. Rev. D* **95** (2017) 071101, [[1612.07818](#)].
 - [74] LHCb collaboration, R. Aaij et al., *Searches for 25 rare and forbidden decays of D^+ and D_s^+ mesons*, *JHEP* **06** (2021) 044, [[2011.00217](#)].
 - [75] NA62 collaboration, E. Cortina Gil et al., *Measurement of the very rare $K^+ \rightarrow \pi^+ \nu \bar{\nu}$ decay*, *JHEP* **06** (2021) 093, [[2103.15389](#)].
 - [76] MICROBOONE collaboration, P. Abratenko et al., *Search for a Higgs Portal Scalar Decaying to Electron-Positron Pairs in the MicroBooNE Detector*, *Phys. Rev. Lett.* **127** (2021) 151803, [[2106.00568](#)].
 - [77] BNL-E949 collaboration, A. V. Artamonov et al., *Study of the decay $K^+ \rightarrow \pi^+ \nu \bar{\nu}$ in the momentum region $140 < P_\pi < 199$ MeV/c*, *Phys. Rev. D* **79** (2009) 092004, [[0903.0030](#)].
 - [78] F. Domingo, *Decays of a NMSSM CP-odd Higgs in the low-mass region*, *JHEP* **03** (2017) 052, [[1612.06538](#)].

- [79] B. R. Holstein, *Allowed eta decay modes and chiral symmetry*, *Phys. Scripta T* **99** (2002) 55–67, [[hep-ph/0112150](#)].
- [80] ATLAS collaboration, M. Aaboud et al., *Search for dark matter in events with a hadronically decaying vector boson and missing transverse momentum in pp collisions at $\sqrt{s} = 13$ TeV with the ATLAS detector*, *JHEP* **10** (2018) 180, [[1807.11471](#)].
- [81] A. Alloul, N. D. Christensen, C. Degrande, C. Duhr and B. Fuks, *FeynRules 2.0 - A complete toolbox for tree-level phenomenology*, *Comput. Phys. Commun.* **185** (2014) 2250–2300, [[1310.1921](#)].
- [82] C. Degrande, C. Duhr, B. Fuks, D. Grellscheid, O. Mattelaer and T. Reiter, *UFO - The Universal FeynRules Output*, *Comput. Phys. Commun.* **183** (2012) 1201–1214, [[1108.2040](#)].
- [83] J. Alwall, R. Frederix, S. Frixione, V. Hirschi, F. Maltoni, O. Mattelaer et al., *The automated computation of tree-level and next-to-leading order differential cross sections, and their matching to parton shower simulations*, *JHEP* **07** (2014) 079, [[1405.0301](#)].
- [84] T. Sjöstrand, S. Ask, J. R. Christiansen, R. Corke, N. Desai, P. Ilten et al., *An introduction to PYTHIA 8.2*, *Comput. Phys. Commun.* **191** (2015) 159–177, [[1410.3012](#)].
- [85] “Lhc higgs cross section working group.”
<https://twiki.cern.ch/twiki/bin/view/LHCPhysics/HiggsEuropeanStrategy>.